NANO LETTERS

pubs.acs.org/NanoLett Letter

ROS-Targeted Depression Therapy via BSA-Incubated Ceria Nanoclusters

Shengyang Fu,[†] Huili Chen,[†] Weitao Yang, Xiaohuan Xia,* Shu Zhao, Xiaonan Xu, Pu Ai, Qingyuan Cai, Xiangyu Li, Yi Wang, Jie Zhu, Bingbo Zhang,* and Jialin C. Zheng*

Cite This: *Nano Lett.* 2022, 22, 4519−4527 Read Online

ACCESS | Metrics & More | Article Recommendations | Supporting Information

ABSTRACT: Depression is one of the most fatal mental diseases, and there is currently a lack of efficient drugs for the treatment of depression. Emerging evidence has indicated oxidative stress as a key pathological feature of depression. We targeted reactive oxygen species (ROS) and synthesized CeO_2@BSA nanoclusters as a novel antidepression nanodrug *via* a convenient, green, and highly effective bovine serum albumin (BSA) incubation strategy. CeO_2@BSA has ultrasmall size (2 nm) with outstanding ROS scavenging and blood-brain barrier crossing capacity, rapid metabolism, and negligible adverse effects *in vitro* and *in vivo*. CeO_2@BSA administration alleviates depressive behaviors and depression-related pathological changes of the chronic restraint stress-induced depressive model, suggesting promising therapeutic effects of CeO_2@BSA for the treatment of depression. Our study proved the validity by directly using nanodrugs as antidepression drugs instead of using them as a nanocarrier, which greatly expands the application of nanomaterials in depression treatment.

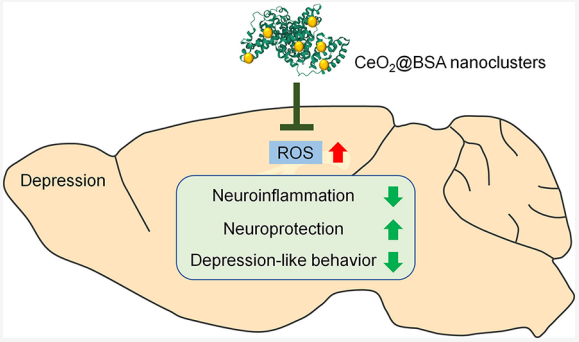

KEYWORDS: *Ceria, depression, reactive oxygen species, bovine serum albumin*

INTRODUCTION

Depression is one of the most common and worldwide mental illnesses with high morbidity and mortality, probably leading to disability or suicide.[1,2] Current therapeutic strategies include psychotherapy, electroconvulsive therapy, and the use of antidepressants, but all with limited outcomes.[3,4] Among all these strategies, the use of antidepressants is the most straightforward and low-stimulative one; however, around 30% of patients with depression do not respond to antidepressant treatment strategies.[5]

The limited therapeutic outcomes after using antidepressants revealed a complicated pathogenesis of depression and the importance of developing non-neurotransmitter pharmaceuticals for depression prevention and treatment. Emerging evidence has indicated oxidative stress and excessive reactive oxygen species (ROS) accumulation as key pathological features of depression, which makes ROS potential therapeutic targets.[6−11] ROS, including hydrogen peroxide, superoxide anion radical, hydroxyl radical, etc., is a term for derivatives of molecular oxygen that are regulated by ROS-generating and consuming enzymes such as peroxidase, nicotinamide adenine dinucleotide phosphate (NADPH), superoxide dismutase (SOD), and catalase (CAT).[12−14] In depression status, the imbalance between ROS production and antioxidative defense induced oxidative stress leads to the dysregulation of brain functions and abnormalities in neuronal signaling processes,[6,15] and supplementation of ROS-inhibiting small molecules has been shown to have a curative effect in depressive patients, such as coenzyme Q10 (CoQ10),[16] ascorbic acid,[17] *N*-acetylcysteine (NAC).[18] Although ROS-targeted depression therapy has shown effectiveness, the conventional antioxidants still have some disadvantages, whether they are small molecules or natural enzymes. For small molecule antioxidants, the antioxidant efficiency is confined due to the consuming reaction and low specificity; natural enzymes exhibit high ROS eliminating efficiency and specificity, but their application is limited due to their high cost, low stability, and difficulty in recycle *in vivo*.[19,20]

Nanozymes are recently developed nanomaterials with enzyme-like activities. Compared with natural enzymes, nanozymes display stronger structural stability, lower cost, higher functional diversity, better catalytic efficiency, recyclability, and feasibility in large-scale preparation.[21,22] There are certain types of nanomaterials with the effective ROS scavenging properties of catalase and superoxide dismutase,

Received: April 4, 2022
Revised: May 12, 2022
Published: May 18, 2022

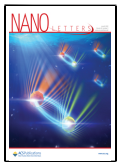

https://doi.org/10.1021/acs.nanolett.2c01334
Nano Lett. 2022, 22, 4519−4527

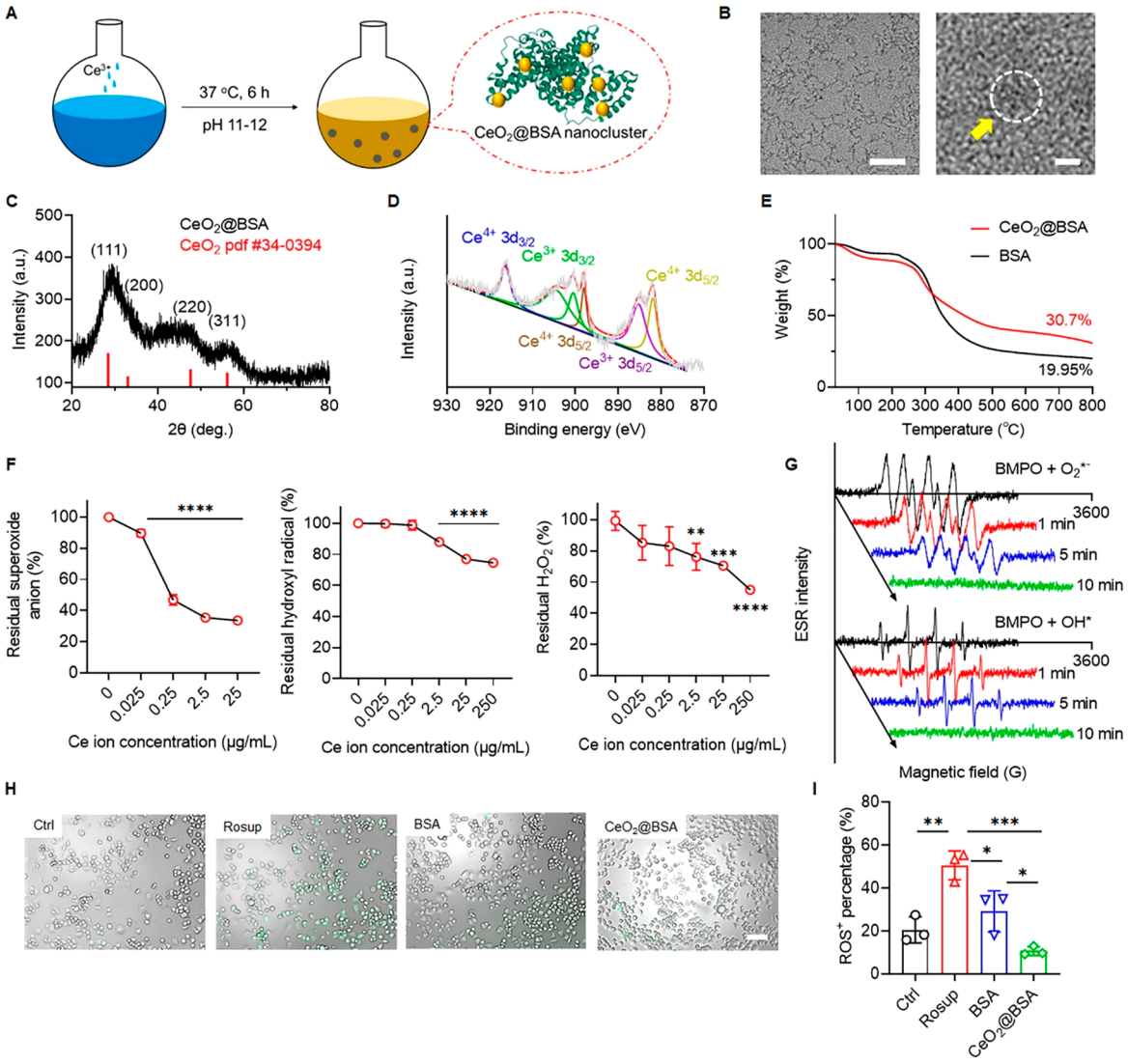

Figure 1. CeO_2@BSA nanoclusters are synthesized *via* a BSA-incubation strategy and can effectively scavenge multiple ROS. (A) Scheme illustration of CeO_2@BSA nanocluster formation. (B) HRTEM images (50 nm for left and 2 nm for right scale bar). (C) XRD and (D) XPS analyses of CeO_2@BSA nanoclusters. (E) TGA analysis of CeO_2@BSA nanoclusters and BSA. Concentration dependent multiple ROS scavenging ability evaluation of CeO_2@BSA nanoclusters, (F) superoxide anion, hydroxyl radical, and hydrogen peroxide. (G) ESR spectrum of time depended free radicals (superoxide anion and hydroxyl radical) scavenging ability of CeO_2@BSA nanoclusters. (H) *In vitro* ROS scavenging ability of CeO_2@BSA nanoclusters in N2a cells (green fluorescence represents ROS) (scale bar: 100 μm) and (I) quantitative analysis (n = 3). Data are shown as mean ± SD. Statistical analysis of (F, I) was performed by one-way ANOVA with a Tukey post hoc test.

including metal oxides and noble metals and compounds.[23−26] Among these nanozymes, nanoceria (CeO_2) is a low-cost one with the property to scavenge multi-ROS *via* the redox reaction by the transition of oxygen vacancies,[23,24,27−29] and it has been used for treating neurological disorders including stroke, Parkinson's disease, and Alzheimer's disease.[30−32] However, these nanocerias still have some defects, such as limited ROS scavenging efficiency, low blood-brain barrier (BBB) penetration efficiency, large size (>5 nm), complicated syntheses process, and extra modifications.[33−35] Therefore, it is urgently necessary to pursue an easy and highly efficient synthesis for preparing ultrasmall metabolizable nanoceria with outstanding ROS scavenging ability and brain accumulation as potential antidepressants.

Herein, nanoceria was synthesized by a convenient, green, and highly effective bovine serum albumin (BSA) incubation strategy, where BSA provided a spatial confinement effect for nanoparticle growth and preventing aggregation.[36−38] BSA has been widely used to synthesize nanoparticles for neurological disorders.[39−41] More importantly, the level of serum albumin decreases in depression patients and high serum albumin levels may provide protection against depression.[42−44] Several key experiments have been performed in solution, *in vitro*, and *in vivo* to assess the ROS scavenging ability, BBB crossing capacity, metabolism, and cytotoxicity of BSA-incubated nanoceria (CeO_2@BSA). The therapeutic effects of CeO_2@BSA nanoclusters were determined using the chronic restraint stress (CRS)-induced depressive model, a more credible depression model to simulate human stress in life, compared with other inflammatory models such as the lipopolysaccharide (LPS)-induced one.[45] Our study proved the validity by directly using nanodrugs as antidepression drugs, acting as a nanocarrier by loading antidepressants,[46,47] which, in turns, greatly

https://doi.org/10.1021/acs.nanolett.2c01334
Nano Lett. 2022, 22, 4519−4527

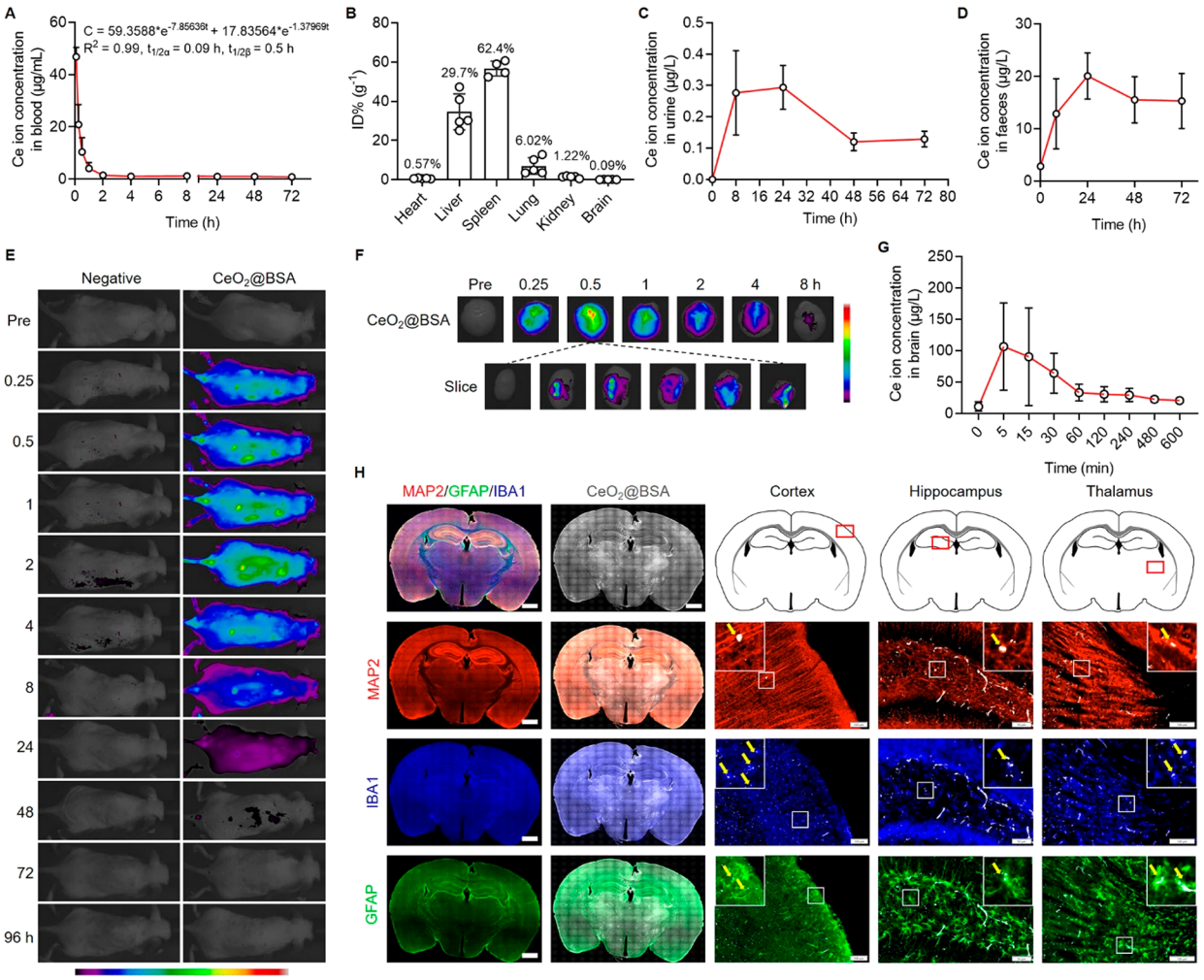

Figure 2. CeO_2@BSA nanoclusters exhibit BBB penetration capacity. (A) *In vivo* blood pharmacokinetics curve. (B) Biodistribution of CeO_2@BSA nanoclusters in major tissues in mice post administration for 30 min. Excreted Ce ion concentration in mouse (C) urine and (D) feces. (E) *In vivo* fluorescence images of control mouse (left) and mouse treated with Cy5-labeled CeO_2@BSA nanoclusters. (F) Fluorescence images of brain tissue post Cy5-labeled CeO_2@BSA nanocluster administration. (G) Ce ion concentration in normal mouse brain (after perfusion). (H) Immunofluorescent staining of mouse brain (MAP2, IBA1, and GFAP for neuron, microglia, and astrocyte, respectively). Scale bar: 1 mm for entire brain slice and 100 μm for the others. Data are shown as mean ± SD.

expands the application of nanomaterials in depression treatment.

RESULTS AND DISCUSSION

CeO_2@BSA was synthesized by a BSA incubation strategy (Figure 1A). Detailed synthetic procedures are elaborated in the Supporting Information. The synthetic method is simple and effective since only three raw materials are utilized in the synthesis process, the synthesis process is green without high temperature and pressure, and the synthetic method can be adapted to mass production. The formation of CeO_2@BSA nanoclusters was characterized by UV−vis spectroscopy, which showed that the absorption peak around 330−340 nm corresponded to Ce−O bonding and that around 280 nm corresponded to BSA[29,36] (Supplementary Figure 1A). The size of CeO_2@BSA could be regulated by different ratios of BSA/Ce^{3+} (Supplementary Table 1, supplementary Figure 1B). CeO_2@BSA nanoclusters were obtained as a clarified buffer solution (Supplementary Figure 2), the size of the nanoclusters was ca. 2 nm in diameter, and the lattice structure was observed *via* transmission electron microscopy (TEM; Figure 1B). X-ray diffracton (XRD) analysis confirmed the formation of CeO_2 crystals, corresponding to the standard of CeO_2 (PDF #34-0394) (Figure 1C). XRD analysis for CeO_2@BSA nanoclusters before and after ROS scavenging reaction suggested no compositional and structural changes of CeO_2@BSA nanoclusters (Supplementary Figure 3). X-ray photoelectron spectroscopy (XPS) analysis confirmed the Ce^{3+} (peaks at 905, 900, and 885 eV) and Ce^{4+} (peaks at 916, 898, and 882 eV), and the ratio of Ce^{3+}/Ce^{4+} reached 0.58, that is attributed to the ROS-scavenging enzymatic activity of CeO_2@BSA nanoclusters[29,31] (Figure 1D). TGA was used to calculate the weight ratio of CeO_2 clusters, and it was found that CeO_2 clusters account for 10% of the weight of CeO_2@BSA nanoclusters (Figure 1E).

To investigate the ROS-scavenging ability of CeO_2@BSA nanoclusters, the levels of representative ROS, superoxide anion, hydroxyl radical, and hydrogen peroxide were studied. For the superoxide anion, CeO_2@BSA nanoclusters showed significant scavenging ability starting at 0.025 μg/mL Ce ion concentration (Figure 1F). Scavenging equilibrium was reached at 25 μg/mL Ce ion concentration, and the scavenging

https://doi.org/10.1021/acs.nanolett.2c01334
Nano Lett. 2022, 22, 4519−4527

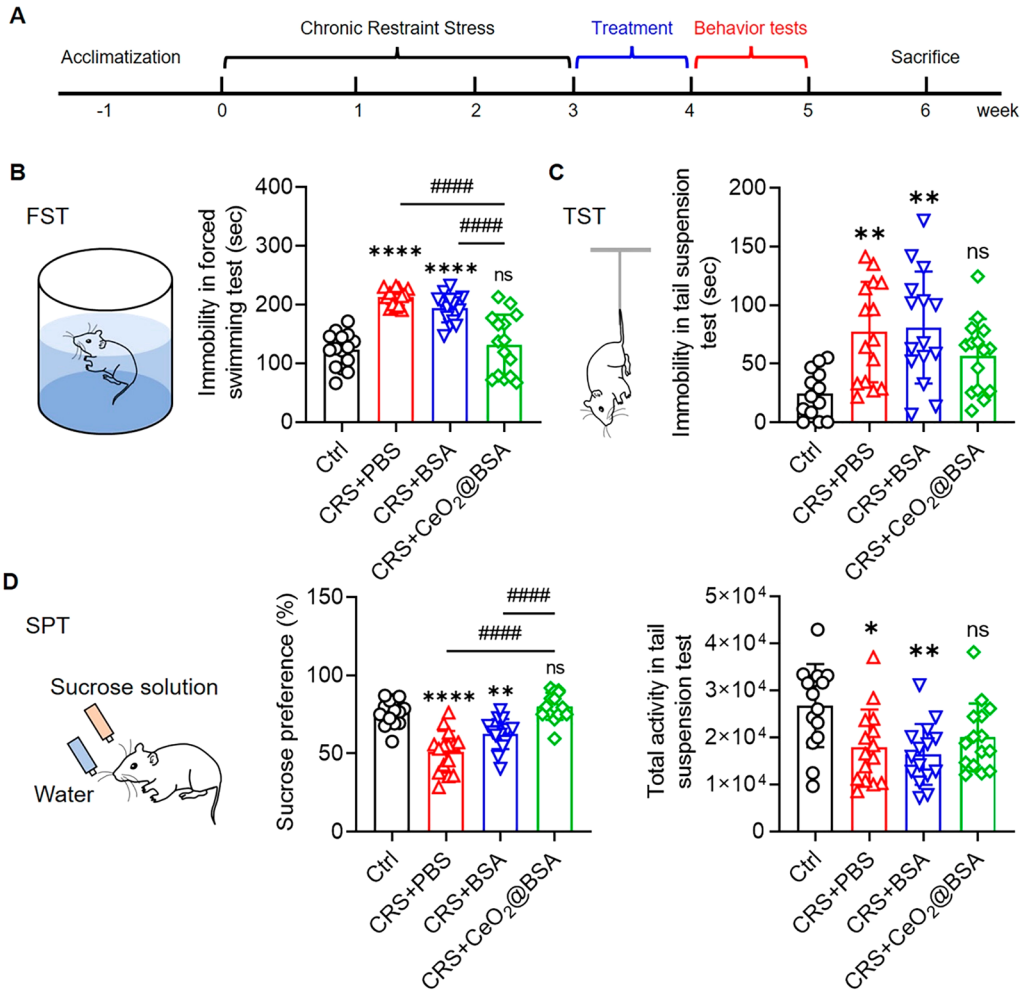

Figure 3. CeO_2@BSA nanoclusters ameliorate depression-like behaviors of CRS mice. (A) Timeline for CRS mice treatment, behavior tests, and pathological ameliorations. Depression-like behavior tests after treatment (n = 15): (B) forced swimming test, (C) sucrose preference test, and (D) tail suspension test. Data are shown as mean ± SD. Statistical analysis was performed by one-way ANOVA with a Tukey post hoc test.

percentage was 66.3% (Figure 1F). For the hydroxyl radical, CeO_2@BSA nanoclusters displayed significant scavenging ability starting at 2.5 μg/mL Ce ion concentration and reached scavenging equilibrium at 250 μg/mL Ce ion concentration (scavenging efficiency of ~15.5%) (Figure 1F). For H_2O_2, CeO_2@BSA nanoclusters showed significant scavenging ability starting at 2.5 μg/mL Ce ion concentration, and the scavenging percentage was 45% at 250 μg/mL Ce ion concentration (Figure 1F). However, due to the insolubility of CeO_2@BSA nanoclusters at concentrations greater than 250 μg/mL Ce ions, the H_2O_2 scavenging equilibrium could not be determined. Electron paramagnetic analyses also proved the rapid superoxide anion, hydroxyl radical-scavenging ability of CeO_2@BSA nanoclusters within 10 min (Figure 1G).

We further characterized the catalytic properties of CeO_2@BSA nanoclusters *via* comparison with a natural antioxidant *N*-acetylcysteine (NAC) (Supplementary Figure 4). NAC significantly restrained superoxide anions during the first and second rounds of reactions but was invalid during the third reaction, while CeO_2@BSA nanocluster was valid in three reactions. During the hydroxyl radical and H_2O_2 scavenging evaluation, the efficiency of NAC was still weaker than that of the CeO_2@BSA nanoclusters in multiple rounds of reactions. These results indicated that the multiple reaction ROS scavenging ability and the catalytic turnovers of CeO_2@BSA nanoclusters are superior to those of the traditional antioxidants.[48] In addition, multiple studies have demonstrated better stability (in a wider range of pH and working temperature) and multiple ROS scavenging ability of nanoceria versus natural enzymes such as SOD and CAT.[28,49] Furthermore, compared with other CeO_2 nanoparticles,[23,32,50] CeO_2@BSA nanoclusters possessed the smallest average size and better ROS scavenging ability (Supplementary Table 2). All these comparisons indicate excellent catalytic property to remove multiple ROS.

To evaluate the intracellular ROS scavenging ability of CeO_2@BSA nanoclusters, Neuro-2a (N2a) cells were pretreated with Rosup to mimic oxidative stress conditions (Figure 1H). The ratio of ROS^+ cells, increased by Rosup treatment (from 21% to 51%), was significantly reduced by the treatment of either BSA (29%) or CeO_2@BSA nanoclusters (11%). Compared with BSA, CeO_2@BSA nanoclusters possessed much better ROS scavenging ability (Figure 1I). These results suggested that the multiple reaction intracellular ROS scavenging ability was mainly attributed to CeO_2 nanoclusters, which is a well-recognized replacement for superoxide dismutase and catalase,[21,51] while BSA contributed to partial ROS scavenging ability, that could be the direct protein oxidation to consume ROS.

https://doi.org/10.1021/acs.nanolett.2c01334
Nano Lett. 2022, 22, 4519−4527

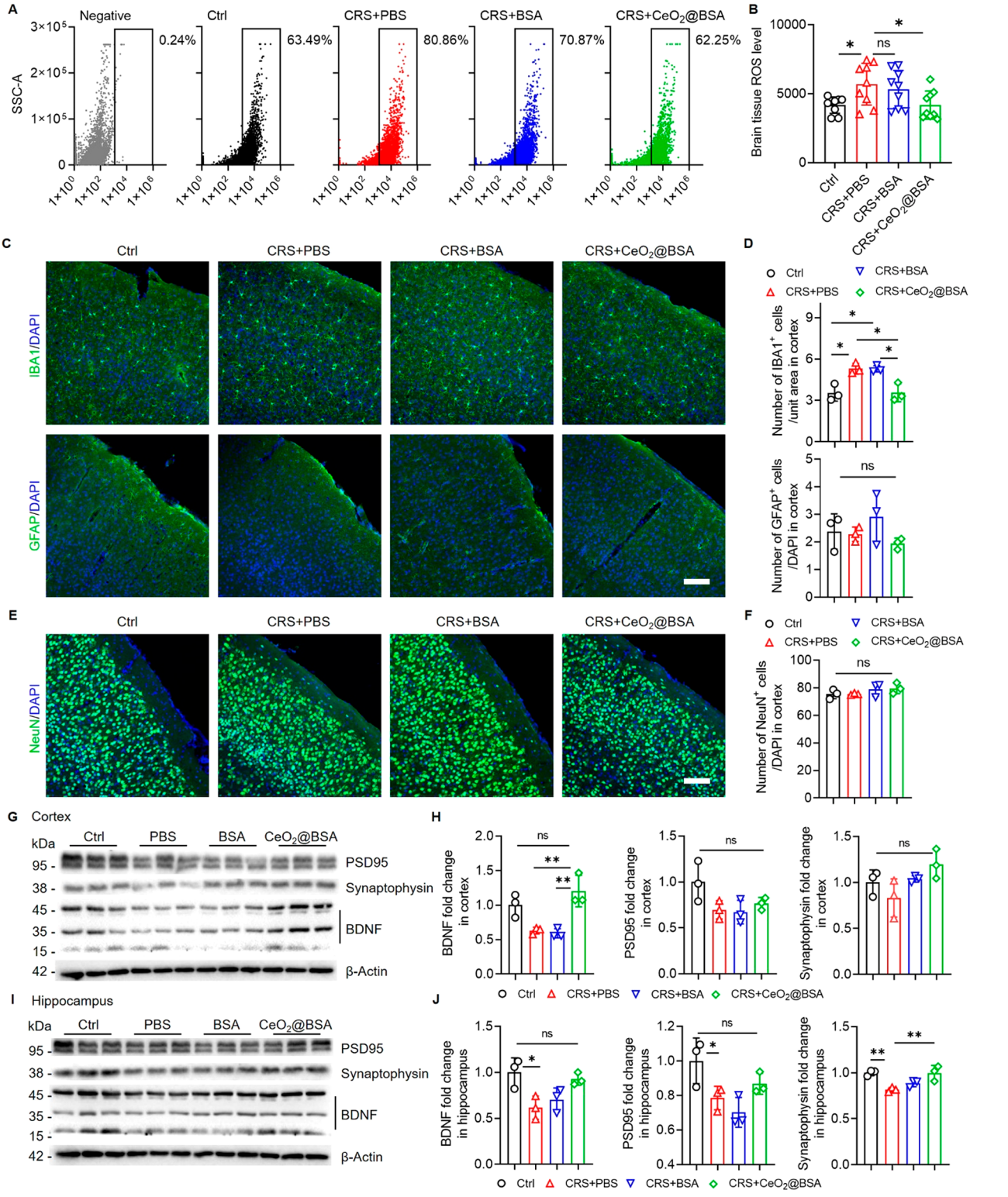

Figure 4. CeO_2@BSA nanocluster administration suppresses ROS accumulation, inhibits microglia activation, and promotes BDNF expression. (A) Flow cytometry detects for brain total ROS in negative, control, and CRS mice treated with PBS, BSA, and CeO_2@BSA nanoclusters. (B) Quantitative comparison of brain ROS levels between control, CRS mice treated with PBS, BSA, and CeO_2@BSA nanoclusters (n = 9). (C) Cortex immunofluorescent staining for IBA1 and GFAP (scale bar: 100 μm) and (D) quantitative results (n = 3). (E) Cortex immunofluorescent staining for NeuN (scale bar: 100 μm) and (F) quantitative result (n = 3). Western blot results of (G) cortex and (I) hippocampus from CRS mice treated with CeO_2@BSA nanoclusters and (H, J) quantitative results (n = 3). Data are shown as mean ± SD. Statistical analysis was performed by one-way ANOVA with a Tukey post hoc test.

The concentration of intravenously injected CeO_2@BSA nanoclusters in mouse blood was matched with a two-compartment pharmacokinetics model (Figure 2A). The half-lives of central and peripheral components were 0.09 and 0.5 h,

https://doi.org/10.1021/acs.nanolett.2c01334
Nano Lett. 2022, 22, 4519−4527

respectively. After PBS perfusion to exclude blood, CeO_2@BSA nanoclusters were found mainly in the spleen (62.4%), liver (29.7%), and lung (6.02%) (Figure 2B). The Ce ion concentration in urine and feces gradually increased, and both reached the highest concentration at 24 h (Figure 2C, D), indicating the metabolizing ability of CeO_2@BSA nanoclusters.

We next verified the BBB crossing ability and the brain accumulation of CeO_2@BSA nanoclusters after intravenous injection. The *in vivo* fluorescence imaging showed that the whole-body distribution of CeO_2@BSA nanoclusters lasted for 24 h (Figure 2E). Moreover, CeO_2@BSA nanoclusters can be found in brain tissues at all tested time points between 0 to 8 h post administration (Figure 2F). In addition, the inductively coupled plasma (ICP) results showed that Ce ions reached the maximum concentration (ca. 106 μg/L) at 5 min and lasted over 600 min after CeO_2@BSA nanocluster administration (Figure 2G). Immunohistochemical analysis revealed homogeneous distribution of CeO_2@BSA nanoclusters that could be detected in $MAP2^+$ neurons, $IBA1^+$ microglia, and $GFAP^+$ astrocytes in the cortex, hippocampus, and thalamus (Figure 2H). Blood-delivered nanoparticles achieved limited accumulation in the brain,[30,31,50] but our results indicate that blood-delivered CeO_2@BSA nanoclusters can cross the BBB and enter brain tissues, which could be attributed to the increased BBB endothelial cell internalization and paracellular permeability of the ultrasmall sized CeO_2@BSA nanoclusters[52,53] and the oxidative-stress- and proinflammatory-cytokine-induced BBB dysfunction in depression.[54,55] It is worth-noting that there are other nanozymes which exhibit anti-ROS capacity (e.g., MnO_2, single-atom catalysts, etc.[50,51,56]) or BBB crossing ability (e.g., Cu_xO, MoS_2, gold nanoparticles, etc.[53,57,58]). Although it is difficult to compare them due to the distinct synthetic methodologies, different working concentrations and conditions, diverse sizes, and ROS removal mechanisms, our results indicate that CeO_2@BSA nanoclusters have both ROS scavenging and BBB crossing capacities, making them a promising nanozyme for the treatment of ROS dysregulation-related neurological disorders including depression.

To evaluate the therapeutic effects of CeO_2@BSA nanoclusters on depression, we first generated mouse depression model by CRS (3 h every day last for 3 weeks) (Supplementary Figure 5A). After restraint, the body weights of CRS mice were significantly lower than those of control mice (Supplementary Figure 5B). CRS mice showed greater immobility in the forced swim test (FST) and tail suspension test (TST) (Supplementary Figure 5C, D) and were less eager for sucrose than control mice (Supplementary Figure 5E). In the open field test (OFT), there was no significant difference in total distance, suggesting no influence of CRS on motor ability (Supplementary Figure 5F). Hence, CRS mice demonstrated typical depressive behaviors. The brain ROS level of CRS mice was measured by flow cytometry. The percentage of ROS^+ cells reached 51.58% in CRS mice, higher than 28.92% in control mice (Supplementary Figure 5G–I), and CRS induced a significant ROS increase (Supplementary Figure 5J). Therefore, our results confirmed the excessive ROS accumulation in depression mouse brains.

CRS mice were then intravenously injected with CeO_2@BSA nanoclusters every other day for 1 week (Figure 3A). In the FST, CeO_2@BSA nanocluster treatment significantly reduced the immobility compared with PBS or BSA treatment (Figure 3B). In the sucrose preference test (SPT), CeO_2@BSA nanocluster treatment recovered the sucrose preference of CRS mice (Figure 3C). In the TST, both the immobility and total activity were rescued by CeO_2@BSA nanocluster treatment with no significant difference from control (Figure 3D). Our results suggested that CeO_2@BSA nanoclusters, but not BSA, ameliorated CRS-induced depression-like behaviors.

Next, we studied the CeO_2@BSA nanocluster-induced pathological changes in CRS mouse brains. Fluorescence activated cell sorting analysis identified 80.86% and 70.87% ROS^+ cells in PBS- and BSA-treated CRS mice, while the proportions of ROS^+ cells for CeO_2@BSA nanocluster treatment and control groups were 62.25% and 63.49%, respectively (Figure 4A). The brain ROS level was significantly decreased in CeO_2@BSA nanocluster treatment group versus PBS group, confirming the ROS elimination capacity of CeO_2@BSA nanoclusters (Figure 4B).

The effects of CeO_2@BSA nanoclusters on glial activation, a potential mechanism of depression,[59,60] were examined next. We found that CeO_2@BSA nanocluster treatment abrogated CRS-induced elevation of $IBA1^+$ activated microglia in the cortex, suggesting an anti-neuroinflammatory effects of CeO_2@BSA nanoclusters under depressive conditions (Figure 4C, D). No difference in the proportions of $GFAP^+$ active astrocytes was observed among all groups, indicating negligible astroglial activation in CRS mouse brains (Figure 4C, D).

We further investigated the neuroprotective functions of CeO_2@BSA nanoclusters. Although we found no difference in the proportions of $NeuN^+$ neurons (Figure 4E, F; Supplementary Figures 6 and 7), CeO_2@BSA nanocluster treatment rescued CRS-induced downregulation of brain derived neurotrophic factor (BDNF) expression in the cortex and hippocampus (Figure 4G–J), that were both downregulated in hippocampus but were increased after CeO_2@BSA nanocluster treatment. Furthermore, CeO_2@BSA nanocluster treatment reversed the downregulated expression levels of presynaptic protein synaptophysin and postsynaptic protein PSD95 in the CRS mouse hippocampus (Figure 4I–J). These results indicate that CeO_2@BSA nanocluster treatment could rescue the expression of BDNF and synaptic proteins in depressive mice.

Lastly, the cytotoxicity of CeO_2@BSA nanoclusters was evaluated in N2a cells, BV2 microglia, and A172 astrocytes. After 24 h of incubation, there was no obvious cytotoxicity within the test concentrations evaluated by CCK8 assay (Supplementary Figure 8, Table 3). Furthermore, CeO_2@BSA nanoclusters were intravenously injected into naïve mice for *in vivo* safety evaluation. Electrocardiograph results did not show an abnormal heart rate in CeO_2@BSA nanocluster-treated mice compared with control mice (Supplementary Figure 9). Routine blood examinations including the numbers of leucocytes, lymphocytes, monocytes, neutrophils, erythrocytes, platelets, and hemoglobin did not show obvious differences between CeO_2@BSA nanocluster-treated mice and control ones (Supplementary Figure 10). The liver and kidney functions of CeO_2@BSA nanocluster-treated mice were in the safe range with no significant difference versus control mice (Supplementary Figures 11 and 12). Importantly, CeO_2@BSA nanocluster treatment did not induce negative emotions as shown by depressive-like behavior tests including TST, FST, and SPT (Supplementary Figure 13). H&E staining indicated no necrosis, congestion, or hemorrhage in the hearts, livers, spleens, lungs, kidneys, and brains (Supplementary Figure 14).

https://doi.org/10.1021/acs.nanolett.2c01334
Nano Lett. 2022, 22, 4519–4527

CONCLUSION

In summary, the concept that oxidative stress serves as a key contributor in the pathogenesis of depression has been widely recognized, and ROS has been proposed as a central target for the next generation antidepressants. Herein, we utilized a recently developed method to synthesize CeO_2@BSA nanoclusters to overcome shortcomings of current anti-ROS natural enzymes and small molecule drugs including antioxidant inefficiency, low stability, high cost, negligible BBB crossing capacity, and difficulty in recycling. More importantly, we demonstrated that CeO_2@BSA nanoclusters could ameliorate depression-like behaviors and depression-related pathological changes like neuroinflammation and the impairment of neuroprotection, almost without negative effects. Our study provides convincing evidence for considering oxidative stress as a therapeutic target of depression, and it will inspire the development of nanodrugs that are directly used as novel antidepressants instead of acting as nanocarriers.

ASSOCIATED CONTENT

Supporting Information

The Supporting Information is available free of charge at https://pubs.acs.org/doi/10.1021/acs.nanolett.2c01334.

Details of CeO_2@BSA nanoclusters synthesis, UV−vis/DLS characterization, the XRD patterns, ROS scavenging ability evaluation, validation of CRS model, pathological changes in hippocampus and amygdala, CeO2@BSA nanoclusters therapeutic and toxicological effects evaluation, experimental materials and methods (PDF)

AUTHOR INFORMATION

Corresponding Authors

Xiaohuan Xia − *Center for Translational Neurodegeneration and Regenerative Therapy, Tongji Hospital affiliated to Tongji University School of Medicine, Shanghai 200065, China; Shanghai Frontiers Science Center of Nanocatalytic Medicine, Tongji University School of Medicine, Shanghai 200331, China; Translational Research Institute of Brain and Brain-Like Intelligence, Shanghai Fourth People's Hospital affiliated to Tongji University School of Medicine, Shanghai 200434, China*; Email: xiaohuan_xia1@163.com

Bingbo Zhang − *The Institute for Translational Nanomedicine, Shanghai East Hospital, Shanghai 200120, China; The Institute for Biomedical Engineering & Nano Science, School of Medicine, Tongji University, Shanghai 200092, China; Shanghai Frontiers Science Center of Nanocatalytic Medicine, Tongji University School of Medicine, Shanghai 200331, China*; orcid.org/0000-0002-0981-7071; Email: bingbozhang@tongji.edu.cn

Jialin C. Zheng − *Center for Translational Neurodegeneration and Regenerative Therapy, Tongji Hospital affiliated to Tongji University School of Medicine, Shanghai 200065, China; The Institute for Biomedical Engineering & Nano Science, School of Medicine, Tongji University, Shanghai 200092, China; Shanghai Frontiers Science Center of Nanocatalytic Medicine, Tongji University School of Medicine, Shanghai 200331, China*; orcid.org/0000-0003-2286-0151; Email: jialinzheng@tongji.edu.cn

Authors

Shengyang Fu − *Center for Translational Neurodegeneration and Regenerative Therapy, Tongji Hospital affiliated to Tongji University School of Medicine, Shanghai 200065, China*

Huili Chen − *Center for Translational Neurodegeneration and Regenerative Therapy, Tongji Hospital affiliated to Tongji University School of Medicine, Shanghai 200065, China*

Weitao Yang − *The Institute for Translational Nanomedicine, Shanghai East Hospital, Shanghai 200120, China; The Institute for Biomedical Engineering & Nano Science, School of Medicine, Tongji University, Shanghai 200092, China; Shanghai Frontiers Science Center of Nanocatalytic Medicine, Tongji University School of Medicine, Shanghai 200331, China*

Shu Zhao − *Center for Translational Neurodegeneration and Regenerative Therapy, Tongji Hospital affiliated to Tongji University School of Medicine, Shanghai 200065, China*

Xiaonan Xu − *Center for Translational Neurodegeneration and Regenerative Therapy, Tongji Hospital affiliated to Tongji University School of Medicine, Shanghai 200065, China*

Pu Ai − *Center for Translational Neurodegeneration and Regenerative Therapy, Tongji Hospital affiliated to Tongji University School of Medicine, Shanghai 200065, China; Wuxi Clinical College of Anhui Medical University, Hefei 230022, China*

Qingyuan Cai − *Center for Translational Neurodegeneration and Regenerative Therapy, Tongji Hospital affiliated to Tongji University School of Medicine, Shanghai 200065, China; Franklin & Marshall College, Lancaster, Pennsylvania 17603, United States*

Xiangyu Li − *Center for Translational Neurodegeneration and Regenerative Therapy, Tongji Hospital affiliated to Tongji University School of Medicine, Shanghai 200065, China*

Yi Wang − *Center for Translational Neurodegeneration and Regenerative Therapy, Yangzhi Rehabilitation Hospital affiliated to Tongji University, Shanghai 200065, China*

Jie Zhu − *Center for Translational Neurodegeneration and Regenerative Therapy, Shanghai Tenth People's Hospital affiliated to Tongji University School of Medicine, Shanghai 200065, China*

Complete contact information is available at: https://pubs.acs.org/10.1021/acs.nanolett.2c01334

Author Contributions

†S.F. and H.C. contributed equally to this work.

Notes

The authors declare no competing financial interest.

ACKNOWLEDGMENTS

This work was supported in part by research grants from the National Natural Science Foundation of China (No. 91949204 and No. 81830037 to J.C.Z., No. 81922035 and No. 81871399 to B.Z., No. 81971145 and No. 81901333 to X.X.), Program of Shanghai Academic Research Leader (20XD1423700 to B.Z.), Shanghai Science and Technology Biomedical Innovation Funds (19441904200 to B.Z.), Shanghai Blue Cross Brain Hospital Co., Ltd., and Shanghai Tongji University Education Development Foundation (No. 000000381/2018108 to J.C.Z.).

https://doi.org/10.1021/acs.nanolett.2c01334
Nano Lett. 2022, 22, 4519−4527

REFERENCES

(1) Wingo, T. S.; Liu, Y.; Gerasimov, E. S.; Gockley, J.; Logsdon, B. A.; Duong, D. M.; Dammer, E. B.; Lori, A.; Kim, P. J.; Ressler, K. J.; Beach, T. G.; Reiman, E. M.; Epstein, M. P.; De Jager, P. L.; Lah, J. J.; Bennett, D. A.; Seyfried, N. T.; Levey, A. I.; Wingo, A. P. Brain proteome-wide association study implicates novel proteins in depression pathogenesis. *Nat. Neurosci* **2021**, *24* (6), 810−817.

(2) Scangos, K. W.; Makhoul, G. S.; Sugrue, L. P.; Chang, E. F.; Krystal, A. D. State-dependent responses to intracranial brain stimulation in a patient with depression. *Nat. Med.* **2021**, *27*, 229−231.

(3) Zhang, C.; Zhang, Y.; Luo, H.; Xu, X.; Yuan, T. F.; Li, D.; Cai, Y. Y.; Gong, H.; Peng, D. H.; Fang, Y. R.; Voon, V.; Sun, B. Bilateral Habenula deep brain stimulation for treatment-resistant depression: clinical findings and electrophysiological features. *Transl Psychiatry* **2022**, *12* (1), 52.

(4) Goldfarb, S.; Fainstein, N.; Ben-Hur, T. Electroconvulsive stimulation attenuates chronic neuroinflammation. *JCI Insight* **2020**, *5* (17), No. e137028.

(5) Kulkarni, S. K; Dhir, A. Current investigational drugs for major depression. *Expert opinion on investigational drugs* **2009**, *18* (6), 767−788.

(6) Bhatt, S.; Nagappa, A. N.; Patil, C. R. Role of oxidative stress in depression. *Drug Discov Today* **2020**, *25* (7), 1270−1276.

(7) Bakunina, N.; Pariante, C. M.; Zunszain, P. A. Immune mechanisms linked to depression via oxidative stress and neuroprogression. *Immunology* **2015**, *144* (3), 365−373.

(8) Ko, S. Y.; Wang, S. E.; Lee, H. K.; Jo, S.; Han, J.; Lee, S. H.; Choi, M.; Jo, H. R.; Seo, J. Y.; Jung, S. J.; Son, H. Transient receptor potential melastatin 2 governs stress-induced depressive-like behaviors. *Proc. Natl. Acad. Sci. U. S. A.* **2019**, *116* (5), 1770−1775.

(9) Ding, Q.; Tian, Y.; Wang, X.; Li, P.; Su, D.; Wu, C.; Zhang, W.; Tang, B. Oxidative damage of tryptophan hydroxylase-2 mediated by peroxisomal superoxide anion radical in brains of mouse with depression. *J. Am. Chem. Soc.* **2020**, *142*, 20735−20743.

(10) Maes, M.; Galecki, P.; Chang, Y. S.; Berk, M. A review on the oxidative and nitrosative stress (O&NS) pathways in major depression and their possible contribution to the (neuro)degenerative processes in that illness. *Prog. Neuropsychopharmacol Biol. Psychiatry* **2011**, *35* (3), 676−92.

(11) Xu, H.; Steven Richardson, J.; Li, X. M. Dose-related effects of chronic antidepressants on neuroprotective proteins BDNF, Bcl-2 and Cu/Zn-SOD in rat hippocampus. *Neuropsychopharmacology* **2003**, *28* (1), 53−62.

(12) Sies, H.; Jones, D. P. Reactive oxygen species (ROS) as pleiotropic physiological signalling agents. *Nat. Rev. Mol. Cell Biol.* **2020**, *21* (7), 363−383.

(13) Prasad, S.; Gupta, S. C.; Tyagi, A. K. Reactive oxygen species (ROS) and cancer: Role of antioxidative nutraceuticals. *Cancer Lett.* **2017**, *387*, 95−105.

(14) Wang, Y.; Branicky, R.; Noe, A.; Hekimi, S. Superoxide dismutases: Dual roles in controlling ROS damage and regulating ROS signaling. *J. Cell Biol.* **2018**, *217* (6), 1915−1928.

(15) Du, R. H.; Wu, F. F.; Lu, M.; Shu, X. D.; Ding, J. H.; Wu, G.; Hu, G. Uncoupling protein 2 modulation of the NLRP3 inflammasome in astrocytes and its implications in depression. *Redox Biol.* **2016**, *9*, 178−187.

(16) Sanoobar, M.; Dehghan, P.; Khalili, M.; Azimi, A.; Seifar, F. Coenzyme Q10 as a treatment for fatigue and depression in multiple sclerosis patients: A double blind randomized clinical trial. *Nutr Neurosci* **2016**, *19* (3), 138−43.

(17) Shivavedi, N.; Kumar, M.; Tej, G.; Nayak, P. K. Metformin and ascorbic acid combination therapy ameliorates type 2 diabetes mellitus and comorbid depression in rats. *Brain Res.* **2017**, *1674*, 1−9.

(18) Nery, F. G.; Li, W.; DelBello, M. P.; Welge, J. A. N-acetylcysteine as an adjunctive treatment for bipolar depression: A systematic review and meta-analysis of randomized controlled trials. *Bipolar Disord* **2021**, *23* (7), 707−714.

(19) Wei, H.; Wang, E. Nanomaterials with enzyme-like characteristics (nanozymes): next-generation artificial enzymes. *Chem. Soc. Rev.* **2013**, *42* (14), 6060−93.

(20) Wang, H.; Wan, K.; Shi, X. Recent advances in nanozyme research. *Adv. Mater.* **2019**, *31* (45), No. 1805368.

(21) Huang, Y.; Ren, J.; Qu, X. Nanozymes: Classification, catalytic mechanisms, activity regulation, and applications. *Chem. Rev.* **2019**, *119* (6), 4357−4412.

(22) Zhang, R.; Yan, X.; Fan, K. Nanozymes inspired by natural enzymes. *Acc. Mater. Res.* **2021**, *2* (7), 534−547.

(23) Weng, Q.; Sun, H.; Fang, C.; Xia, F.; Liao, H.; Lee, J.; Wang, J.; Xie, A.; Ren, J.; Guo, X.; Li, F.; Yang, B.; Ling, D. Catalytic activity tunable ceria nanoparticles prevent chemotherapy-induced acute kidney injury without interference with chemotherapeutics. *Nat. Commun.* **2021**, *12* (1), 1436.

(24) Yu, H.; Jin, F.; Liu, D.; Shu, G.; Wang, X.; Qi, J.; Sun, M.; Yang, P.; Jiang, S.; Ying, X.; Du, Y. ROS-responsive nano-drug delivery system combining mitochondria-targeting ceria nanoparticles with atorvastatin for acute kidney injury. *Theranostics* **2020**, *10* (5), 2342−2357.

(25) Sancho-Albero, M.; Rubio-Ruiz, B.; Pérez-López, A. M.; Sebastián, V.; Martín-Duque, P.; Arruebo, M.; Santamaría, J.; Unciti-Broceta, A. Cancer-derived exosomes loaded with ultrathin palladium nanosheets for targeted bioorthogonal catalysis. *Nat. Catal* **2019**, *2*, 864−872.

(26) Ge, C.; Fang, G.; Shen, X.; Chong, Y.; Wamer, W. G.; Gao, X.; Chai, Z.; Chen, C.; Yin, J.-J. Facet energy versus enzyme-like activities: The unexpected protection of palladium nanocrystals against oxidative damage. *ACS Nano* **2016**, *10* (11), 10436−10445.

(27) Sun, Y.; Sun, X.; Li, X.; Li, W.; Li, C.; Zhou, Y.; Wang, L.; Dong, B. A versatile nanocomposite based on nanoceria for antibacterial enhancement and protection from aPDT-aggravated inflammation via modulation of macrophage polarization. *Biomaterials* **2021**, *268*, 120614.

(28) Matter, M. T.; Furer, L. A.; Starsich, F. H. L.; Fortunato, G.; Pratsinis, S. E.; Herrmann, I. K. Engineering the bioactivity of flame-made ceria and ceria/bioglass hybrid nanoparticles. *ACS Appl. Mater. Interfaces* **2019**, *11* (3), 2830−2839.

(29) Kalashnikova, I.; Chung, S.-J.; Nafiujjaman, M.; Hill, M. L.; Siziba, M. E.; Contag, C. H.; Kim, T. Ceria-based nanotheranostic agent for rheumatoid arthritis. *Theranostics* **2020**, *10* (26), 11863−11880.

(30) Hegazy, M. A. E.; Maklad, H. M.; Abd Elmonsif, D. A.; Elnozhy, F. Y.; Alqubiea, M. A.; Alenezi, F. A.; Al abbas, O. M.; Al abbas, M. M. The possible role of cerium oxide (CeO2) nanoparticles in prevention of neurobehavioral and neurochemical changes in 6-hydroxydopamine-induced parkinsonian disease. *Alexandria J. Med.* **2019**, *53* (4), 351−360.

(31) Choi, S. W.; Kim, J. Recent progress in autocatalytic ceria nanoparticles-based translational research on brain diseases. *ACS Applied Nano Materials* **2020**, *3*, 1043−1062.

(32) Kim, C. K.; Kim, T.; Choi, I. Y.; Soh, M.; Kim, D.; Kim, Y. J.; Jang, H.; Yang, H. S.; Kim, J. Y.; Park, H. K.; Park, S. P.; Park, S.; Yu, T.; Yoon, B. W.; Lee, S. H.; Hyeon, T. Ceria nanoparticles that can protect against ischemic stroke. *Angew. Chem., Int. Ed. Engl.* **2012**, *51* (44), 11039−43.

(33) Bai, X.; Wang, S.; Yan, X.; Zhou, H.; Zhan, J.; Liu, S.; Sharma, V. K.; Jiang, G.; Zhu, H.; Yan, B. Regulation of cell uptake and cytotoxicity by nanoparticle core under the controlled shape, size, and surface chemistries. *ACS Nano* **2020**, *14* (1), 289−302.

(34) Ma, X.; Wu, Y.; Jin, S.; Tian, Y.; Zhang, X.; Zhao, Y.; Yu, L.; Liang, X.-J. Gold nanoparticles induce autophagosome accumulation through size-dependent nanoparticle uptake and lysosome impairment. *ACS Nano* **2011**, *5* (11), 8629−8639.

(35) Liu, T.; Xiao, B.; Xiang, F.; Tan, J.; Chen, Z.; Zhang, X.; Wu, C.; Mao, Z.; Luo, G.; Chen, X.; Deng, J. Ultrasmall copper-based nanoparticles for reactive oxygen species scavenging and alleviation of inflammation related diseases. *Nat. Commun.* **2020**, *11* (1), 2788.

https://doi.org/10.1021/acs.nanolett.2c01334
Nano Lett. 2022, 22, 4519−4527

(36) Saif, B.; Gu, Q.; Yang, P. The synthesis of protein-encapsulated ceria nanorods for visible-light driven hydrogen production and carbon dioxide reduction. *Small* **2021**, *17*, No. 2103422.
(37) Yang, W.; Guo, W.; Chang, J.; Zhang, B. Protein/peptide-templated biomimetic synthesis of inorganic nanoparticles for biomedical applications. *J. Mater. Chem. B* **2017**, *5* (3), 401−417.
(38) Zhang, B.; Wang, J.; Yu, J.; Fang, X.; Wang, X.; Shi, D. Site-specific biomimetic precision chemistry of bimodal contrast agent with modular peptides for tumor-targeted imaging. *Bioconjug Chem.* **2017**, *28* (2), 330−335.
(39) Hou, W.; Jiang, Y.; Xie, G.; Zhao, L.; Zhao, F.; Zhang, X.; Sun, S. K.; Yu, C.; Pan, J. Biocompatible BSA-MnO2 nanoparticles for in vivo timely permeability imaging of blood-brain barrier and prediction of hemorrhage transformation in acute ischemic stroke. *Nanoscale* **2021**, *13* (18), 8531−8542.
(40) Lamichhane, S.; Lee, S. Albumin nanoscience: Homing nanotechnology enabling targeted drug delivery and therapy. *Arch Pharm. Res.* **2020**, *43* (1), 118−133.
(41) Xu, K.; Zhao, Z.; Zhang, J.; Xue, W.; Tong, H.; Liu, H.; Zhang, W. Albumin-stabilized manganese-based nanocomposites with sensitive tumor microenvironment responsivity and their application for efficient SiRNA delivery in brain tumors. *J. Mater. Chem. B* **2020**, *8* (7), 1507−1515.
(42) Van Hunsel, F.; Wauters, A.; Vandoolaeghe, E.; Neels, H.; Demedts, P.; Maes, M. Lower total serum protein, albumin, and beta- and gamma-globulin in major and treatment-resistant depression: Effects of antidepressant treatments. *Psychiatry Res.* **1996**, *65*, 159−169.
(43) Maes, M.; De Vos, N.; Demedts, P.; Wauters, A.; Neels, H. Lower serum zinc in major depression in relation to changes in serum acute phase proteins. *J. Affective Disord.* **1999**, *56*, 189−194.
(44) Poudel-Tandukar, K.; Jacelon, C. S.; Bertone-Johnson, E. R.; Palmer, P. H.; Poudel, K. C. Serum albumin levels and depression in people living with Human Immunodeficiency Virus infection: a cross-sectional study. *J. Psychosom Res.* **2017**, *101*, 38−43.
(45) Planchez, B.; Surget, A.; Belzung, C. Animal models of major depression: drawbacks and challenges. *J. Neural Transm (Vienna)* **2019**, *126* (11), 1383−1408.
(46) Liu, Y.; Hu, P.; Zheng, Z.; Zhong, D.; Xie, W.; Tang, Z.; Pan, B.; Luo, J.; Zhang, W.; Wang, X. Photoresponsive vaccine-like CAR-M system with high-efficiency central immune regulation for inflammation-related depression. *Adv. Mater.* **2021**, *34*, e2108525.
(47) Jin, L.; Hu, P.; Wang, Y.; Wu, L.; Qin, K.; Cheng, H.; Wang, S.; Pan, B.; Xin, H.; Zhang, W.; Wang, X. Fast-acting black-phosphorus-assisted depression therapy with low toxicity. *Adv. Mater.* **2019**, *32* (2), e1906050.
(48) Zandieh, M.; Liu, J. Nanozyme catalytic turnover and self-limited reactions. *ACS Nano* **2021**, *15* (10), 15645−15655.
(49) Zhou, X.; Zeng, W.; Rong, S.; Lv, H.; Chen, Y.; Mao, Y.; Tan, W.; Li, H. Alendronate-modified nanoceria with multiantioxidant enzyme-mimetic activity for reactive oxygen species/reactive nitrogen species scavenging from cigarette smoke. *ACS Appl. Mater. Interfaces* **2021**, *13* (40), 47394−47406.
(50) Kwon, H. J.; Cha, M. Y.; Kim, D.; Kim, D. K.; Soh, M.; Shin, K.; Hyeon, T.; Mook-Jung, I. Mitochondria-targeting ceria nanoparticles as antioxidants for Alzheimer's disease. *ACS Nano* **2016**, *10* (2), 2860−70.
(51) Cao, F.; Zhang, L.; You, Y.; Zheng, L.; Ren, J.; Qu, X. An enzyme-mimicking single-atom catalyst as an efficient multiple reactive oxygen and nitrogen species scavenger for sepsis management. *Angew. Chem., Int. Ed. Engl.* **2020**, *59* (13), 5108−5115.
(52) Liang, J.; Zhu, Y.; Gao, C.; Ling, C.; Qin, J.; Wang, Q.; Huang, Y.; Lu, W.; Wang, J. Menthol-modified BSA nanoparticles for glioma targeting therapy using an energy restriction strategy. *NPG Asia Mater.* **2019**, *11* (1), 38.
(53) Gao, N.; Dong, K.; Zhao, A.; Sun, H.; Wang, Y.; Ren, J.; Qu, X. Polyoxometalate-based nanozyme: Design of a multifunctional enzyme for multi-faceted treatment of Alzheimer's disease. *Nano Research* **2016**, *9*, 1079−1090.
(54) Welcome, M. O. Cellular mechanisms and molecular signaling pathways in stress-induced anxiety, depression, and blood-brain barrier inflammation and leakage. *Inflammopharmacology* **2020**, *28* (3), 643−665.
(55) Wu, S.; Yin, Y.; Du, L. Blood-brain barrier dysfunction in the pathogenesis of major depressive disorder. *Cell Mol. Neurobiol.* **2021**, DOI: 10.1007/s10571-021-01153-9.
(56) Zhang, Y.; Khalique, A.; Du, X.; Gao, Z.; Wu, J.; Zhang, X.; Zhang, R.; Sun, Z.; Liu, Q.; Xu, Z.; Midgley, A. C.; Wang, L.; Yan, X.; Zhuang, J.; Kong, D.; Huang, X. Biomimetic design of mitochondria-targeted hybrid nanozymes as superoxide scavengers. *Adv. Mater.* **2021**, *33* (9), e2006570.
(57) Ren, C.; Li, D.; Zhou, Q.; Hu, X. Mitochondria-targeted TPP-MoS2 with dual enzyme activity provides efficient neuroprotection through M1/M2 microglial polarization in an Alzheimer's disease model. *Biomaterials* **2020**, *232*, 119752.
(58) Ma, M.; Liu, Z.; Gao, N.; Pi, Z.; Du, X.; Ren, J.; Qu, X. Self-protecting biomimetic nanozyme for selective and synergistic clearance of peripheral amyloid-beta in an Alzheimer's disease model. *J. Am. Chem. Soc.* **2020**, *142*, 21702−21711.
(59) Yirmiya, R.; Rimmerman, N.; Reshef, R. Depression as a microglial disease. *Trends Neurosci* **2015**, *38* (10), 637−658.
(60) Cao, P.; Chen, C.; Liu, A.; Shan, Q.; Zhu, X.; Jia, C.; Peng, X.; Zhang, M.; Farzinpour, Z.; Zhou, W.; Wang, H.; Zhou, J. N.; Song, X.; Wang, L.; Tao, W.; Zheng, C.; Zhang, Y.; Ding, Y. Q.; Jin, Y.; Xu, L.; Zhang, Z. Early-life inflammation promotes depressive symptoms in adolescence via microglial engulfment of dendritic spines. *Neuron* **2021**, *109* (16), 2573−2589.

https://doi.org/10.1021/acs.nanolett.2c01334
Nano Lett. 2022, 22, 4519−4527